Citation: Cell Death and Disease (2012) 3, e434; doi:10.1038/cddis.2012.173

www.nature.com/cddis

Targeting β-tubulin:CCT-β complexes incurs Hsp90- and VCP-related protein degradation and induces ER stress-associated apoptosis by triggering capacitative Ca^{2+} entry, mitochondrial perturbation and caspase overactivation

Y-F Lin[1], Y-F Lee[2] and P-H Liang*[,1,2]

We have previously demonstrated that interrupting the protein–protein interaction (PPI) of β-tubulin:chaperonin-containing TCP-1β (CCT-β) induces the selective killing of multidrug-resistant cancer cells due to CCT-β overexpression. However, the molecular mechanism has not yet been identified. In this study, we found that CCT-β interacts with a myriad of intracellular proteins involved in the cellular functions of the endoplasmic reticulum (ER), mitochondria, cytoskeleton, proteasome and apoptosome. Our data show that the targeted cells activate both the heat-shock protein 90 (Hsp90)-associated protein ubiquitination/degradation pathway to eliminate misfolded proteins in the cytoplasm and the valosin-containing protein (VCP)-centered ER-associated protein degradation pathway to reduce the excessive levels of unfolded polypeptides from the ER, thereby mitigating ER stress, at the onset of β-tubulin:CCT-β complex disruption. Once ER stress is expanded, ER stress-associated apoptotic signaling is enforced, as exhibited by cellular vacuolization and intracellular Ca^{2+} release. Furthermore, the elevated intracellular Ca^{2+} levels resulting from capacitative Ca^{2+} entry augments apoptotic signaling by provoking mitochondrial perturbation and caspase overactivation in the targeted cells. These findings not only provide a detailed picture of the apoptotic signaling cascades evoked by targeting the β-tubulin:CCT-β complex but also demonstrate a strategy to combat malignancies with chemoresistance to Hsp90- and VCP-related anticancer agents.

Cell Death and Disease (2012) **3,** e434; doi:10.1038/cddis.2012.173; published online 29 November 2012
Subject Category: Cancer

Chaperonin-containing TCP-1 (CCT) is a hetero-oligomeric ring complex composed of eight subunits (α, β, γ, δ, ε, ζ, η, and θ).[1] The eukaryotic CCT primarily assists with the protein assembly of *de novo* unfolded polypeptides, such as the cytoskeleton components, actin and tubulin, and the cell cycle regulators, cyclin E and Cdc20, in an ATP-dependent manner.[2,3] Depletion of the CCT complex appears to perturb both microfilament- and microtubule-based cytoskeleton activity without interfering with actin and tubulin polypeptide synthesis,[4,5] and the complex also affects the protein networks required for the morphogenesis and survival of sensory neurons, thereby promoting neurodegenerative diseases.[6] Therefore, the CCT complex acts as a protein-folding machine in the maintenance of cellular homeostasis.

Recently, increased levels of CCT subunits, such as CCT-β, CCT-ε and CCT-ζ, were found to be associated with the tumorigenesis of hepatocellular and colorectal cancers.[7–9] Moreover, we found that cancer cells with multidrug resistance (MDR) abundantly express the CCT-β subunit and that disrupting the protein–protein interaction (PPI) of CCT-β with its protein substrate, β-tubulin, with a synthetic *N*-iodoacetyl-tryptophan (I-Trp) preferentially kills the MDR cancer cells via a caspase-dependent apoptotic mechanism.[10] This approach represents a novel strategy to combat MDR cancer cells. In this study, we aim to investigate further the molecular mechanism by which the PPI blocker (e.g., I-Trp) of the β-tubulin:CCT-β complex triggers caspase-dependent cell apoptosis in the targeted cells.

As reported in this study, we performed a pull-down assay to identify the PPI networks of CCT-β in the target cells and found that CCT-β constitutively interacts with heat-shock protein 90 (Hsp90) and the valosin-containing protein (VCP)-associated ubiquitin proteasome system (UPS), as well as proteins required for protein synthesis and Ca^{2+} regulation in the endoplasmic reticulum. Our data show that targeting β-tubulin:CCT-β complexes with I-Trp stimulates target cells

[1]Institute of Biological Chemistry, Academia Sinica, Taipei 11529, Taiwan, ROC and [2]Institute of Biochemical Sciences, National Taiwan University, Taipei 10617, Taiwan, ROC
*Corresponding author: P-H Liang, Institute of Biological Chemistry, Academia Sinica, 128 Academia Road, Taipei 11529, Taiwan, ROC. Tel: +886 2 2366 5539 ext. 3091; Fax: +886 2 2363 5038; E-mail: phliang@gate.sinica.edu.tw
Edited by H-U Simon
Keywords: capacitative Ca^{2+} entry; β-tubulin; CCT-β; caspases; apoptosis
Abbreviations: I-Trp, *N*-iodoacetyl-tryptophan; CCT, chaperonin-containing TCP-1; ER, endoplasmic reticulum; Hsp90, heat-shock protein 90; VCP, valosin-containing protein
Received 18.6.12; revised 21.9.12; accepted 16.10.12; Edited by H-U Simon

to activate Hsp90- and VCP-dependent UPS rapidly to mitigate ER stress.[11,12] This I-Trp-induced perturbation of the protein networks originating from the disruption of β-tubulin:CCT-β complexes apparently triggers both protein degradation systems, thereby forcing target cells towards ER stress-associated apoptosis. In this pathway, the elevated intracellular Ca^{2+} levels and mitochondrial destruction ultimately converge to overactivate the caspases involved in apoptosis. This report is the first to describe the apoptotic mechanism evoked by targeting the β-tubulin:CCT-β complex. Furthermore, this mechanism provides insight into the PPI of CCT-β with Hsp90 and VCP, which both represent potential anticancer targets.[13,14]

Results

CCT-β is crucial for I-Trp-induced cell apoptosis. Using mass spectrometric analysis, we have previously found that I-Trp binds to β-tubulin by alkylating the Cys^{354} residue, thereby disrupting the β-tubulin:CCT-β complex and inducing cell apoptosis.[10] However, the detailed molecular mechanism remains unclear (Figure 1a). To confirm whether the alkylation of residue Cys^{354} is the key step for interrupting the PPI of the β-tubulin:CCT-β complex and inducing apoptosis, we generated variant human embryonic kidney (HEK)-293 cell lines that stably express exogenous plasmids either without (mock) or with DNA encoding either wild-type (wt) or mutant (C354S) β-tubulin. The HEK-293 cells were selected because they express high levels of the β-tubulin and CCT-β proteins (Supplementary Figure 1) and are thus highly sensitive to I-Trp.[10] Western blot analysis revealed that β-tubulin levels were relatively abundant in HEK-293 cells expressing either wt or C354S β-tubulin compared with the control cells, whereas the CCT-β expression levels were comparable among the three variants (Figure 1b). The overexpression of wt β-tubulin dramatically enhanced I-Trp-induced apoptosis in HEK-293 cells, while the expression of C354S β-tubulin inhibited this effect (Figure 1c), thereby indicating that I-Trp interrupted the PPI of the β-tubulin:CCT-β complex[10] by alkylating the Cys^{354} residue. The experiments showing that wt and C354S β-tubulin-expressing HEK-293 cells exhibited a comparable sensitivity to tubulin-binding agent paclitaxel (PTX)[15]-induced G2M arrest (Supplementary Figure 2a) and intrinsic apoptotic pathway inducer staurosporine[16]-caused sub-G0 cell accumulation (Supplementary Figure 2b) supports this statement. In contrast, we also generated stable HEK-293 cell lines artificially expressing either non-target (CTL) shRNA (as a control) or CCT-β shRNA to analyze the role that CCT-β has in I-Trp-induced cell apoptosis. Compared with the parental and control cells, HEK-293 cells expressing CCT-β shRNA displayed a dramatic reduction in CCT-β expression without affecting β-tubulin expression (Figure 1d). The reduction in CCT-β expression levels significantly rendered the HEK-293 cells resistant to I-Trp-induced cell apoptosis (Figure 1e). Similar results were also observed in the MDR MES-SA/Dx5 cells.[10] Unlike the results obtained with tubulin-binding agents (e.g., PTX), our data demonstrate that the binding

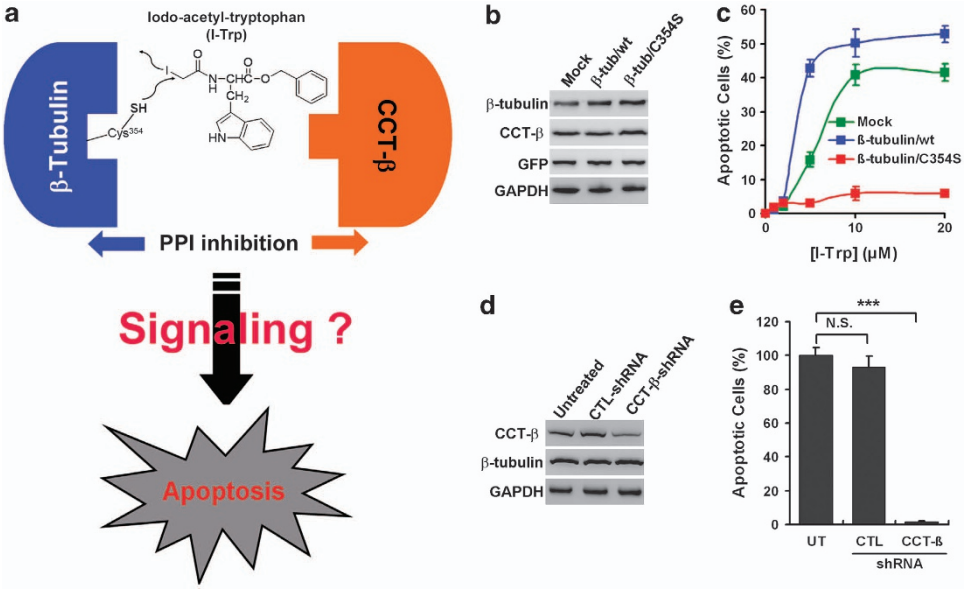

Figure 1 The importance of alkylating the β-tubulin Cys^{354} residue and CCT-β expression in I-Trp-induced cell apoptosis. (**a**) Interrupting PPI of β-tubulin:CCT-β by I-Trp leads to cell apoptosis. (**b**) The expression levels of β-tubulin, CCT-β, green fluorescent protein (GFP) and glyceraldehyde 3-phosphate dehydrogenase (GAPDH) in the HEK-293 cell lysates expressing the pIRES2-EGFP plasmid DNA either without (mock) or with wild-type β-tubulin (β-tub/wt) or C354S mutant (β-tub/C354S) were assessed by immunoblotting with the corresponding antibodies. (**c**) Incorporation of I-Trp into β-tubulin Cys^{354} is required for eliciting apoptosis of HEK-293 cells. The cells were treated with I-Trp at the indicated concentrations. Apoptosis was measured 24 h after treatment. (**d**) The expression levels of CCT-β, β-tubulin and GAPDH were analyzed by western blotting using specific antibodies for the HEK-293 cell lysates either untreated or treated with stably expressing control (CTL) or CCT-β shRNA. (**e**) Knockdown of CCT-β inhibits I-Trp-induced apoptosis of HEK-293 cells. Cells were treated with I-Trp at 5 μM. Apoptosis was assessed 24 h after treatment. GFP was used as CTL for the transfection procedure. GAPDH was used as protein loading CTL. The results in (**c**) and (**e**) represent the mean of three independent experiments. The values shown represent the mean ± S.D. The symbol '***' denotes statistical significance at $P<0.001$. NS represents results that are not significant

of I-Trp to β-tubulin did not alter the dynamics of the microtubule.[10] These data indicate that CCT-β might have a crucial role in mediating I-Trp-induced apoptosis once the β-tubulin:CCT-β complex is disrupted. Therefore, we next assessed the involvement of CCT-β-associated proteins in cell apoptosis induced by disrupting the β-tubulin:CCT-β complex.

Identification of intracellular CCT-β-associated proteins. To isolate the proteins constitutively associated with CCT-β, we first purified N-terminal His-tagged CCT-β recombinant protein as the bait (Supplementary Figure 3a). Next, we performed immunoprecipitation analysis to validate the binding ability of the His-tagged CCT-β protein with its protein substrate, β-tubulin, *in vitro* (Supplementary Figure 3b). Based on these results, we performed a pull-down experiment with recombinant CCT-β protein with cell lysates derived from HEK-293, parental MES-SA or MDR MES-SA/Dx5 cells, and subsequently analyzed the proteins that were pulled down by electrophoresis (Supplementary Figure 3c). We excised the major protein bands, as indicated from the gel, and examined them via mass spectrometric analysis (Supplementary Figure 3c). Using Mascot software to analyze the mass spectrometric data against the NCBI human protein database, we identified several proteins (Figure 2a) that may be associated with CCT-β. As expected, the cytoskeleton proteins, actin and tubulin, which are both well-known protein substrates of CCT and capable of interacting with CCT-β, were identified from protein band B. With protein band A, we found Hsp90 and its homologous proteins, tumor necrosis factor type 1 receptor-associated protein and tumor rejection antigen (gp96), which are located in the mitochondria and ER, respectively. These proteins are referred to as chaperones or stress proteins because they exhibit a critical function in assisting newly synthesized polypeptides (clients) in achieving functional conformation, localization, activation and oligomerization.[17] The proteasome subunit p26, which participates in the cytoplasmic UPS and is responsible for the proteolytic degradation of misfolded proteins,[18] was also identified from protein band B. VCP, which has a critical role in ER-associated protein degradation (ERAD) machinery and couples with its cofactors, Ufd1-Npl4, to dislodge misfolded/polyubiquitinated proteins, including misfolded Hsp90 clients, by a retrotranslocation model from the ER into the cytoplasm for degradation by the UPS in response to ER stress,[19] was identified from protein band A. With protein band B, we identified SPFH-1, which is a recognition protein of the inositol 1,4,5-trisphosphate (IP_3) receptors, forms tetrameric calcium channels in the ER membrane, controls the release

a

Protein ID	Protein Name	M.W.	Mascot Score	Biochemical Function/ Intracellular Distribution	Protein Bands
gi|4501881	actin	41.77	516	Cytoskeleton/Cytoplasm	B
gi|340021	tubulin	50.12	85	Cytoskeleton/Cytoplasm	B
gi|4503483	eukaryotic translation elongation factor 2	95.28	194	Translation/Endoplasmic Reticulum	A
gi|7765076	S3 ribosomal protein	26.70	156	Translation/Endoplasmic Reticulum	C
gi|61656607	tumor rejection antigen (gp96)	92.28	110	ER hsp96 chaperone/Endoplasmic Reticulum	A
gi|6005721	SPFH1	37.82	72	ER-Associated Protein Degradation/ Endoplasmic Reticulum	B
gi|6005942	valosin-containing protein (VCP)	89.27	279	ER-Associated Protein Degradation / Cytoplasm	A
gi|687239	tumor necrosis factor type 1 receptor associated protein (TRAP-1)	93.86	146	Mitochondrial hsp90 chaperone/Mitochondria	A
gi|1184320	X-linked inhibitor of apoptosis protein (XIAP)	56.66	231	Anti-apoptosis/Cytoplasm	B
gi|4502581	caspase 7 isoform alpha precursor	34.23	73	Apoptosis/Cytoplasm	C
gi|20149594	90kDa heat shock protein-beta	83.24	769	Cytosolic hsp90 chaperone/Cytoplasm	A
gi|195539395	proteosome 26S	45.77	82	Ubiquitin-Proteosome System/Cytoplasm	B

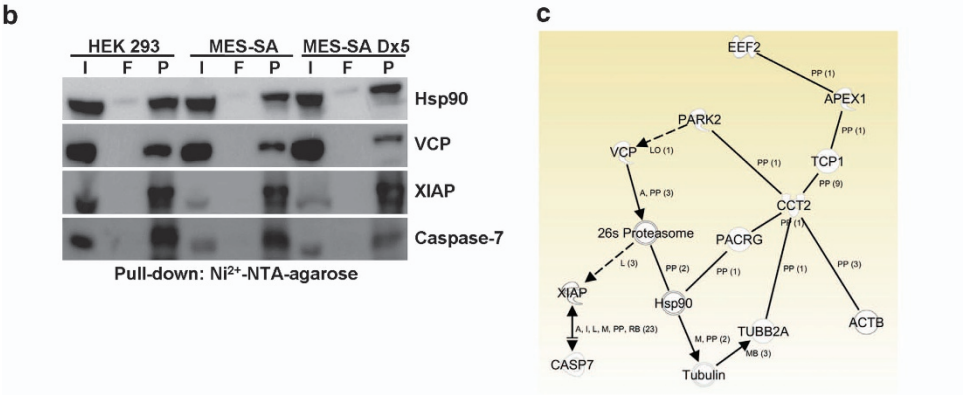

Figure 2 The PPI networks of CCT-β. (**a**) Mass spectrometric analysis of the CCT-β-interacting proteins that were pulled down from HEK-293 cells. (**b**) CCT-β interacts with Hsp90, VCP, XIAP and caspase-7 during the resting stage of target cells. Total cell lysates (input, I), proteins from the flow-through (F) and pellets (P) in the pull-down assay of CCT-β from cell lysates derived from HEK-293, MES-SA and MES-SA/Dx5 cells were analyzed by western blotting with Hsp90, VCP, XIAP and caspase-7 antibodies. (**c**) The PPI network of CCT-β (CCT2) as analyzed using the IPA software. The symbol 'pp' denotes protein–protein interaction. Solid and dashed lines represent direct and indirect interactions, respectively. NTA, nitrilotriacetic acid

of ER Ca^{2+} stores and intimately associates with VCP-centered ERAD machinery to regulate the protein degradation of IP_3 receptors expressed on the ER membrane.[20] The protein translational regulators, eukaryotic translation elongation factor 2 (EEF2) and S3 ribosomal protein, were also identified from protein bands A and C, respectively. Interestingly, in protein band B, we identified X-linked inhibitor of apoptosis protein (XIAP), which exerts antiapoptotic effects by confining active caspase-3, caspase-7 and caspase-9,[21] and is capable of relieving ER stress-induced apoptosis.[22] Moreover, caspase-7, which is one of executioner caspases involved in the demolition phase of apoptosis[23] and has been considered to be closely associated with ER stress-induced apoptosis,[24] was found in protein band C. To confirm the results obtained from the mass spectrometric analysis, we performed immunoblotting to detect Hsp90, VCP, XIAP and caspase-7 using the corresponding antibodies in the mixture of proteins identified in the CCT-β pull-down with HEK-293, MES-SA or MES-SA/Dx5 cells. Our data revealed that CCT-β is probably constitutively coupled with these proteins in the target cells (Figure 2b). To understand further the PPI of CCT-β with the identified proteins in the public domains, we performed a network assessment of CCT-β using the Ingenuity Pathway Analysis (IPA) (http://www.ingenuity.com). The results demonstrated that CCT-β directly interacts with the β-subunits of actin and tubulin and indirectly affects both Hsp90- and VCP-related proteasome activities. Moreover, CCT-β was shown to couple with the ER system via a connection with the EEF2 pathway (Figure 2c). Although the IPA results did not support the hypothesis that CCT-β directly interacts with XIAP and caspase-7, the activation of the proteasome due to the destruction of the β-tubulin:CCT-β complex may trigger the proteolysis of XIAP, thereby relieving XIAP inhibition of caspase-7 activity during cell apoptosis.

Overall, in the resting stage, CCT-β probably interacts with molecules that have a role in assisting protein assembly, eliminating misfolded proteins via the UPS or ERAD machinery and governing ER functions. Therefore, we proposed the hypothesis that targeting the β-tubulin:CCT-β complex with I-Trp presumably interferes with the PPI of CCT-β with those molecules, which might sequentially activate Hsp90- and VCP-associated UPS activities and provoke an ER stress-dependent cell apoptosis in the target cells.

Destruction of the β-tubulin:CCT-β complex provokes Hsp90-dependent protein ubiquitination and degradation. To test our hypothesis, we examined whether Hsp90 chaperone activity is altered in response to I-Trp stimulation. It has been shown that Hsp90 collaborates with Hsp70 and other co-chaperones to assist protein folding of its clients or convey misfolded/ubiquitinated proteins to the UPS for terminally proteolytic degradation.[17] Recently, this Hsp70/Hsp90 protein folding complex was reported to interact with the CCT multi-subunit complex via an interaction with its β-subunit, CCT-β.[25] To understand the role of Hsp90 in the cellular apoptosis induced by the β-tubulin:CCT-β complex destruction, we generated an Hsp90 knockdown variant using HEK-293 cells. Remarkably, silencing Hsp90 expression (Figure 3a) suppressed I-Trp-induced cell apoptosis in HEK-293 cells (Figure 3b). Moreover, I-Trp treatment caused a massive deposition of ubiquitinated proteins, but was relieved by reducing CCT-β expression by stably producing CCT-β shRNA in HEK-293 cells (Figure 3c). Our data also show that disrupting the β-tubulin:CCT-β complex results in a rapid elevation in intracellular proteasome activity, while inhibiting Hsp90 chaperone activity with geldanamycin (GA) led to a moderate elevation in proteasome activity (Figure 3d) within several minutes post-treatment. The knockdown of Hsp90 expression markedly suppressed I-Trp-induced proteasomal activation in comparison with untreated and control shRNA-expressing cells (Figure 3e). These data indicate that targeting the β-tubulin:CCT-β complex with I-Trp might inhibit Hsp90 activity in the protein trafficking of its clients, for example, β-tubulin,[26] to the CCT complex, while activating the Hsp90-associated UPS activity.

Interrupting the β-tubulin:CCT-β complex recruits the VCP-centered ERAD machinery. We next determined whether the VCP-centered ERAD pathway is recruited in response to I-Trp stimulation. It has been shown that VCP is required for extracting unfolded/misfolded proteins from the ER to mitigate ER stress[27] and that loss of VCP function or expression consequently leads to an ER stress-dependent cell apoptosis.[28] Therefore, we artificially overexpressed VCP in HEK-293 cells (Figure 4a) to determine whether increased VCP expression compromised I-Trp-induced cell apoptosis. Our data show that overexpression of VCP significantly suppressed I-Trp-induced apoptosis of HEK-293 cells compared with the parental and control cells (Figure 4b). Conversely, the inhibition of VCP activity with its pharmaceutical inhibitor synergistically enhanced the cytotoxic effects of I-Trp on HEK-293 cells (Figure 4c). Moreover, similar to silencing VCP expression with siRNA,[28] I-Trp treatment caused cellular vacuolization (Figure 4d), which is a characteristic of the elevation of ER stress.[28] Conversely, overexpression of VCP reduced the I-Trp-caused cellular vacuolization (Figure 4d). To further clarify the elevation of ER stress in response to I-Trp treatment, we determined the gene expression of XBP1 (an ER stress marker)[29] and CCTβ-associated molecules, VCP, Hsp90, β-actin, β-tubulin, XIAP and caspase-7 (Figure 4e and Supplementary Figure 4). Our data show that I-Trp increases mRNA levels of XBP1, VCP, Hsp90 and CCTβ (Figure 4e), as well as XIAP (Supplementary Figure 4) in HEK-293 cells within 4 h post-treatment. However, mRNA levels of other CCTβ-associated molecules, β-actin, β-tubulin and caspase-7, were not affected by I-Trp treatment (Supplementary Figure 4). These findings demonstrate that the VCP-centered ERAD pathway is indeed activated but might be overloaded in the event of counteracting the elevated ER stress, due to the deposition of unfolded proteins that resulted from the I-Trp-induced disruption of the β-tubulin:CCT-β complex. As ER stress is continuously expanded, the targeted cells might be committed to ER stress-associated apoptosis.

β-tubulin:CCT-β complex disruption evokes intracellular Ca^{2+} mobilization via the capacitative Ca^{2+} entry model. We then examined the occurrence of ER stress-associated apoptotic signaling cascades in I-Trp-treated

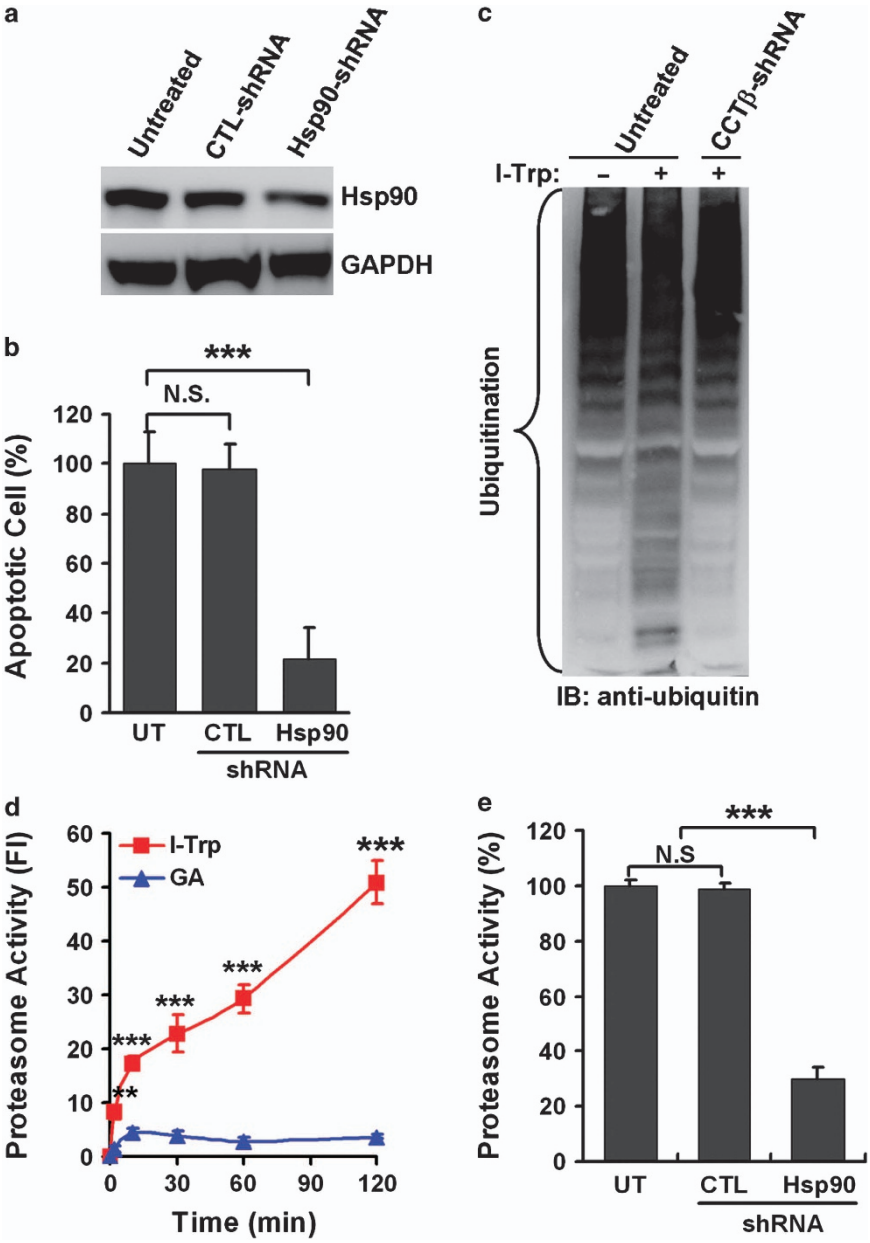

Figure 3 The activation of Hsp90-associated UPS in response to I-Trp treatment. (**a**) The protein levels of Hsp90 and glyceraldehyde 3-phosphate dehydrogenase (GAPDH) were determined in cell lysates from HEK-293 cells either untreated or treated with stably expressing control (CTL) or Hsp90 shRNA by western blot analysis using specific antibodies. (**b**) The knockdown of Hsp90 inhibits I-Trp-induced apoptosis in HEK-293 cells. After treatment with I-Trp (5 μM) for 24 h, cell apoptosis was assessed via PI-based flow cytometric analysis. (**c**) Destruction of the β-tubulin:CCT-β complex with I-Trp induces intracellular protein ubiquitination. Cell lysates from HEK-293 cells either untreated or treated with stably expressing CCT-β shRNA were collected 24 h after I-Trp (5 μM) treatment and immunoblotted (IB) with anti-ubiquitin antibodies. (**d**) Targeting the β-tubulin:CCT-β complex with I-Trp incurs Hsp90-associated proteasome activity. HEK-293 cells were treated with either I-Trp (5 μM) or GA (1 μM) for the designated time periods. Cell lysates were examined using the proteasome activity assay. (**e**) HEK-293 cells either untreated or treated with stably expressing CTL or Hsp90 shRNA were treated with I-Trp (5 μM) for 2 h. Cell lysates were then analyzed for proteasome activity. The results in (**b**), (**d**) and (**e**) are the mean of three independent experiments. The values shown represent the mean ± S.D. The symbols '**' and '***' denote statistical significances at $P<0.001$ and $P<0.01$, respectively. NS represents results that are not significant

cells. Intracellular Ca^{2+} release from the ER often occurs in the expansion of ER stress to amplify the apoptotic signaling.[30] To determine whether interrupting the β-tubulin:CCT-β complex evokes intracellular Ca^{2+} mobilization, a living cell-based Ca^{2+} image analysis was performed in HEK-293 cells. The data revealed that the treatment with I-Trp evoked a rapid intracellular Ca^{2+} elevation reaching a maximal Ca^{2+} level within 60 s, which was sustained for 180 s and declined after 240 s (Supplementary Movie 1 and Figure 5a, top), whereas iodoacetamide (IDAM) (used as a control) failed to evoke intracellular Ca^{2+} mobilization in HEK-293 cells (Supplementary Movie 2 and Figure 5a, bottom). To delineate whether the I-Trp-induced intracellular Ca^{2+} elevation was a consequence of intracellular Ca^{2+}

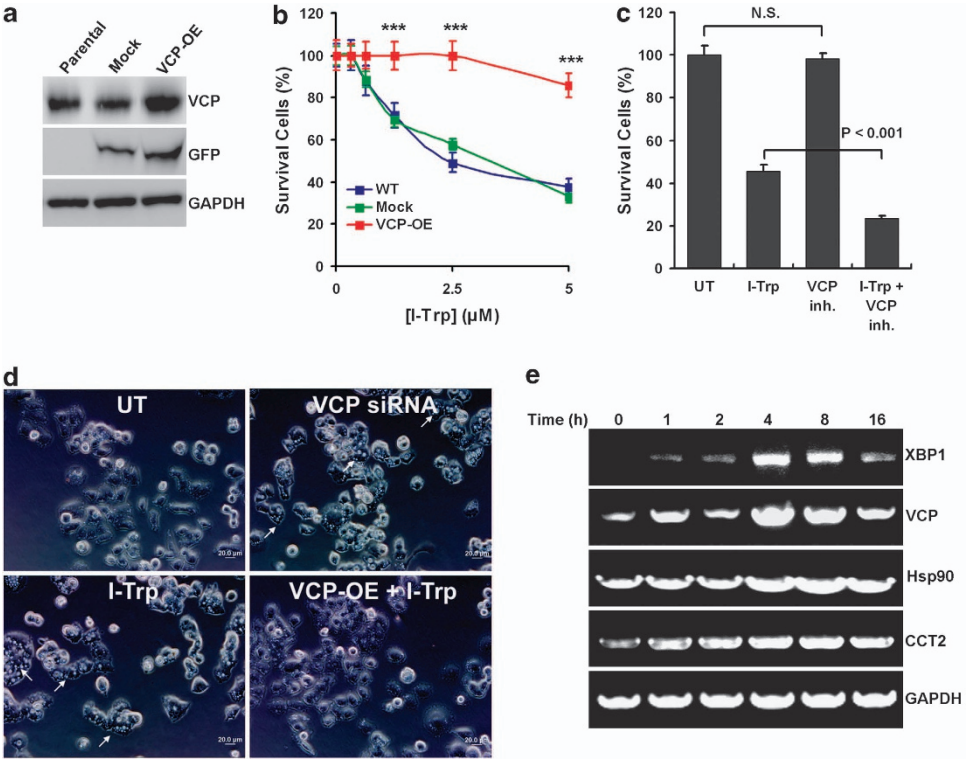

Figure 4 The recruitment of VCP-centered ERAD pathway following β-tubulin:CCT-β complex disruption with I-Trp. (**a**) The expression levels of VCP, green fluorescent protein (GFP) and glyceraldehyde 3-phosphate dehydrogenase (GAPDH) were determined by western blot analysis using specific antibodies in the cell lysates from parental HEK-293 cells or HEK-293 cells expressing pIRES2-EGFP plasmid DNA either without (mock) or with the *VCP* gene. GFP was used as control for the transfection procedure. GAPDH was used as protein loading control. (**b**) Overexpression of VCP compromises I-Trp-induced apoptosis in HEK-293 cells. Parental (WT) HEK-293 cells or HEK-293 cells overexpressing (OE) pIRES2-EGFP plasmid DNA either without (mock) or with the *VCP* gene (VCP-OE) were treated with I-Trp (5 μM) for 24 h, and cell apoptosis was assessed by PI-based flow cytometric analysis. (**c**) The inhibition of VCP activity enhances I-Trp-induced apoptosis of HEK-293 cells. Cells were pre-treated either without (UT) or with the VCP inhibitor (VCP inh.) at 10 μM for 1 h before the treatment without (UT) or with I-Trp (5 μM) for 24 h. Cell apoptosis was assessed by PI-based flow cytometric analysis. (**d**) The disruption of the β-tubulin:CCT-β complex using I-Trp causes cellular vacuolization in HEK-293 cells. Cells were untreated, transfected with VCP siRNA for 24 h or cells without or with VCP overexpression were treated with I-Trp (5 μM) for 2 h. Cellular vacuolization (indicated by arrows) was examined under the microscope. The bars denote a length of 20 μM in diameter. (**e**) Cells were treated with I-Trp at 5 μM for indicated time periods. The mRNA levels of XBP1, VCP, Hsp90, CCTβ and GAPDH were analyzed by RT-PCR using their paired primers. GAPDH was used as an internal control. The results in (**b**) and (**c**) are the mean of three independent experiments. The values shown represent the mean ± S.D. The symbol '***' denotes statistical significance at $P<0.001$. NS represents results that are not significant

release from the ER store, a Fura-2-based intracellular Ca^{2+} assessment of HEK-293 cells was performed in the absence of extracellular Ca^{2+} supplement. The data show that I-Trp immediately evoked an intracellular Ca^{2+} oscillation in the absence of extracellular Ca^{2+} supplement, thereby causing a large increase in Ca^{2+} levels as a result of extracellular Ca^{2+} replenishment (Figure 5b, left), whereas the treatment with IDAM failed to elicit an increase in intracellular Ca^{2+} levels in HEK-293 cells (Figure 5b, middle). Thapsigargin (TG), which inactivates the Ca^{2+}-ATPase pump to achieve Ca^{2+} release from the ER store following a voltage-operated Ca^{2+} channel-dependent extracellular Ca^{2+} entry, which is referred to as the capacitative Ca^{2+} entry model,[31] readily evoked intracellular Ca^{2+} oscillation, as was observed with I-Trp in HEK-293 cells (Figure 5b, right). Pharmaceutical inhibition of intracellular Ca^{2+} release with dantrolene (DTL)[32] (Figure 5c) or chelating intracellular Ca^{2+} ions with 1,2-bis(o-aminophenoxy)ethane-*N*,*N*,*N*′,*N*′-tetraacetic acid (BAPTA)-AM[33] (Figure 5d) remarkably prevented the I-Trp-induced apoptosis of HEK-293 cells. The relief of ER stress might partially contribute to the reduced cell apoptosis as pre-treatment with DTL obviously repressed the mRNA expression of ER stress marker XBP1 (Figure 5e) and stress-related molecules VCP and Hsp90 (Supplementary Figure 5) in I-Trp-treated cells. These findings suggest that intracellular Ca^{2+} mobilization functions to relay ER stress-associated apoptotic signals in response to β-tubulin:CCT-β complex disruption. However, the inhibition of ER Ca^{2+} release by DTL did not change the mRNA level of CCTβ (Supplementary Figure 5), implying that I-Trp-induced CCTβ upregulation might be modulated by other cellular mechanism.

Caspase overactivation in the event of β-tubulin:CCT-β destruction. We have previously demonstrated that the destruction of the β-tubulin:CCT-β complex elicits the over-activation of intracellular caspases, except caspase-1, thereby inducing cellular apoptosis.[10] As intracellular Ca^{2+} release has been shown to be essential for caspase-3 and caspase-9 activation,[34] we next attempted to delineate the effect of intracellular Ca^{2+} release evoked by β-tubulin:CCT-β complex disruption on caspase overactivation in HEK-293

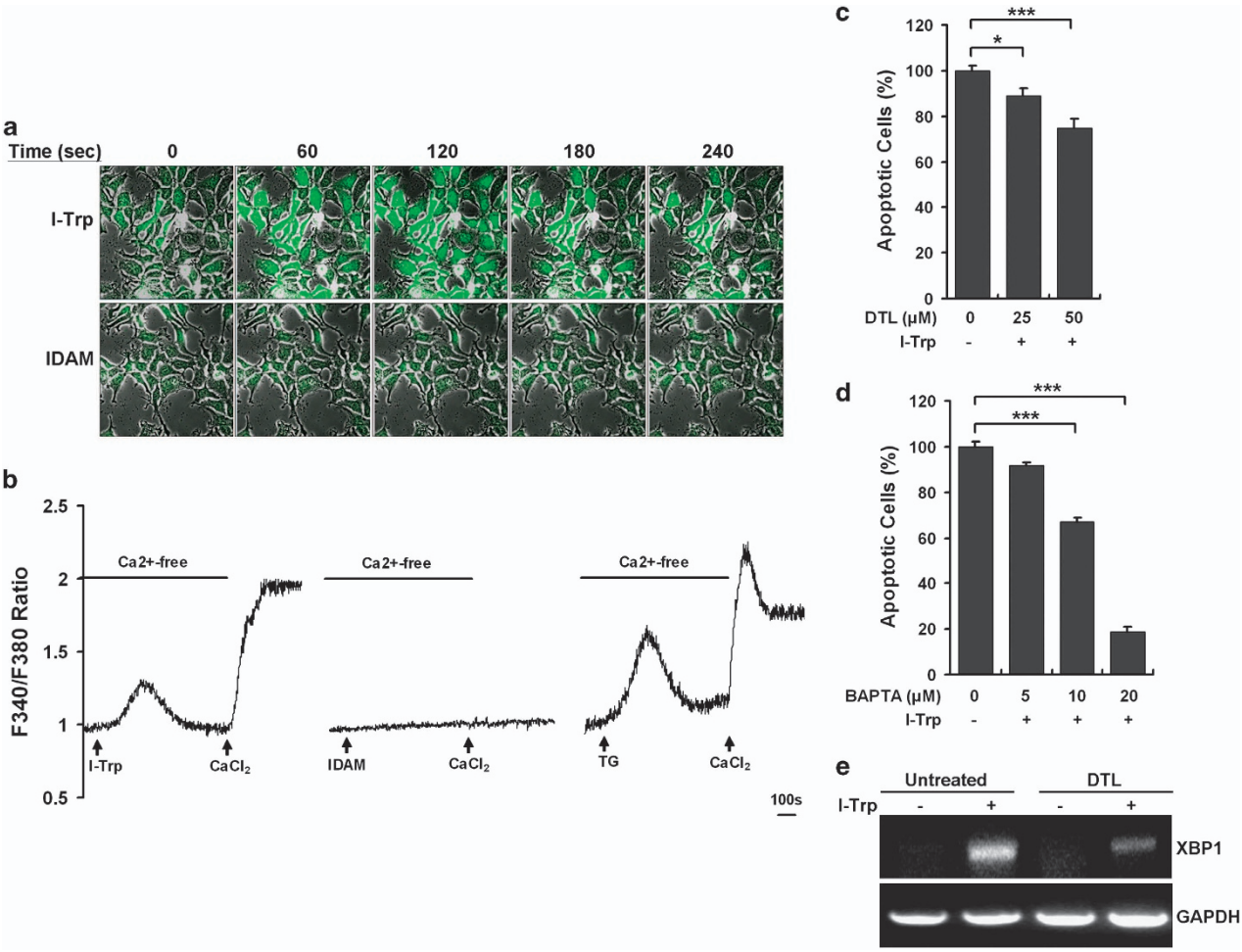

Figure 5 The disruption of the β-tubulin:CCT-β complex using I-Trp evokes capacitative Ca^{2+} entry in HEK-293 cells. (**a**) I-Trp induces intracellular Ca^{2+} mobilization. HEK-293 cells were pre-incubated with Fluoro-3 (4 μM) for 30 min before the treatment with either I-Trp or IDAM (5 μM of each). The changes in the intracellular fluorescent intensities indicate the increased Ca^{2+} levels and were recorded every 5 s and documented as animation movies (Supplementary Movies) using a confocal microscope. The figures shown represent the alterations in the intracellular Ca^{2+} levels post-treatment with either I-Trp or IDAM at the indicated time courses. (**b**) The intracellular Ca^{2+} mobilization induced by I-Trp functions via the capacitative Ca^{2+} entry model in HEK-293 cells. The cells were pre-incubated with Fura-2-AM (5 μM) for 30 min, and the intracellular Ca^{2+} levels were subsequently assessed. Next, 5 μM I-Trp (right), 5 μM IDAM (middle) or 1 μM TG (left) was added (arrows) to the cells bathed in Ca^{2+}-free focal buffer to detect intracellular Ca^{2+} release after starting the Ca^{2+} level measurements. Calcium chloride ($CaCl_2$) (100 μM) was then added (arrows) to the external media to determine the extracellular Ca^{2+} influx. The changes in intracellular Ca^{2+} levels are presented with the ratio of Fura-2 fluorescent intensities at 510 nm emitted by dual excitation wavelengths at 340 nm (Ca^{2+}-bound) and 380 nm (Ca^{2+}-free). (**c**) The evoked intracellular Ca^{2+} mediates I-Trp-induced apoptosis in HEK-293 cells. The cells were pre-treated with the intracellular Ca^{2+} release inhibitor, DTL, at the indicated doses for 30 min before the treatment with 5 μM I-Trp. Cell apoptosis was assessed 24 h post-treatment. (**d**) HEK-293 cells were pre-incubated with the cell-permeable Ca^{2+} chelator, BAPTA, at the indicated concentrations for 30 min. Cell apoptosis was then determined 24 h after I-Trp (5 μM) treatment. (**e**) Cells were pre-treated without or with DTL (50 μM) for 30 min before the treatment without or with I-Trp (5 μM) for 4 h. The mRNA levels of XBP1 and glyceraldehyde 3-phosphate dehydrogenase (GAPDH) were analyzed by RT-PCR using their paired primers. GAPDH was used as an internal control. The results in (**c**) and (**d**) are the mean of three independent experiments. The values shown represent the mean ± S.D. The symbol '*' and '***' denote statistical significance at $P<0.05$ and $P<0.001$, respectively

cells. We treated the cells with TG to induce an intracellular Ca^{2+} release directly and subsequently examined the intracellular caspase activity. The activity levels of initiator caspases, caspase-2, caspase-4, caspase-5, caspase-8 and caspase-10, as well as the effector caspases, caspase-3 and caspase-7, were significantly increased, while the activity level of initiator caspase-9 was slightly elevated in the TG-treated HEK-293 cells (Figure 6a). However, the activity levels of the effector caspase-6 and caspase-1 were not detectable throughout the TG administration in HEK-293 cells (Figure 6a). The pharmaceutical inhibition of intracellular Ca^{2+} release with DTL exhibited a dose-dependent reduction in the activity levels of the initiator caspases, caspase-4, caspase-5, caspase-8 and caspase-10, induced by I-Trp treatment (Figure 6b). These data reveal that the elevated intracellular Ca^{2+} levels have an important role in the activation of the caspase family during I-Trp-induced cell apoptosis.

Mitochondrial perturbation in response to β-tubulin:CCT-β destruction. Mitochondrial perturbation occurs either after TG-induced intracellular Ca^{2+} release from the

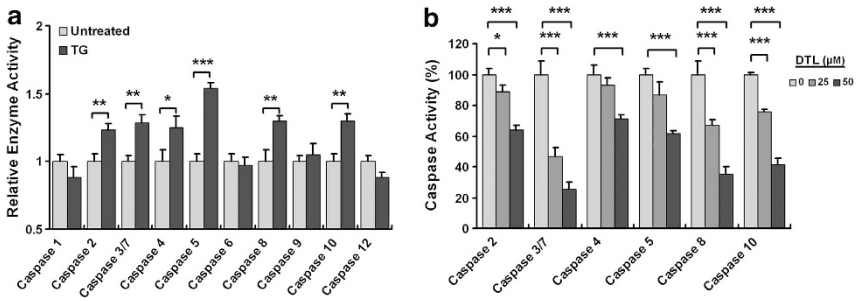

Figure 6 Caspase overactivation occurs upon Ca^{2+} mobilization induced by I-Trp in HEK-293 cells. (**a**) Cells were treated with 1 μM TG for 24 h. After the incubation period, the cell lysates were collected and analyzed using a caspase activity assay. (**b**) The cells were pre-treated with DTL at the indicated concentrations before the treatment with 5 μM I-Trp. The activity levels of caspase-2, caspase-3/7, caspase-4, caspase-5, caspase-8 and caspase-10 were assessed 24 h after I-Trp treatment. The results in (**a**) and (**b**) are the mean of three independent experiments. Values shown represent the mean ± S.D. The symbols '*', '**' and '***' denote statistical significance at $P<0.05$, $P<0.01$ and $P<0.001$, respectively

ER[35] or upon the activation of caspase-8[36] and is critical for triggering the intrinsic caspase-9-dependent apoptotic pathway. Therefore, we next examined whether mitochondrial perturbation takes place in I-Trp-treated HEK-293 cells. The data show that treatment with I-Trp altered the mitochondrial membrane potential (Figure 7a) and induced cytochrome *c* release from the mitochondria to the cytoplasm in a dose- (Figure 7b) and time- (Figure 7c) dependent manner. Fluorescent immunocytological staining revealed that treatment with I-Trp caused mitochondrial disruption and cytochrome *c* release (Figure 7d). Silencing CCT-β expression predominantly abolished cytochrome *c* release from the mitochondria in I-Trp-treated cells (Figure 7e). Accordingly, the inhibition of intracellular Ca^{2+} release with DTL (Figure 7f) and inhibition of caspase-8 activity with its peptide inhibitor, IETD (Figure 7g), markedly suppressed cytochrome *c* release from the mitochondria. These findings indicate that I-Trp-induced ER Ca^{2+} release and caspase-8 activation modulate mitochondrial perturbation and cytochrome *c* release, which might, in turn, trigger intrinsic caspase-9-dependent caspase activation during cell apoptosis in the target cells.

Discussion

In this study, we show that disrupting the intracellular β-tubulin:CCT-β complex with I-Trp by alkylating the Cys^{354} residue of β-tubulin activates the Hsp90/UPS pathway to elicit cellular proteolysis; however, this disruption probably impedes the protein trafficking of Hsp90 clients (e.g., β-tubulin[26]) from the ER compartment to the CCT complex,[25] thereby promoting the accumulation of unfolded proteins in the ER compartment and amplifying ER stress. Although the VCP-centered ERAD pathway is concurrently activated to extract unfolded proteins from the ER to mitigate the elevated ER stress, ER stress-associated cell apoptosis is eventually enforced in the target cells. The Ca^{2+} release from the ER is likely to be crucial for relaying I-Trp-induced ER stress-associated cell apoptosis, as the elevated Ca^{2+} levels via the capacitative Ca^{2+} entry model are required to trigger mitochondrial perturbation, cytochrome *c* release and caspase overactivation (Figure 8).

Hsp90 expression has been found to correlate with tumorigenesis and cancer progression,[37,38] and the protein serves as novel chemotherapeutic target for cancer therapy.[14] Therefore, compromising Hsp90 function with the corresponding inhibitors, such as GA and tanespimycin (17-AAG), has become a promising anticancer strategy to combat certain malignances.[39,40] However, acquired chemoresistance of the Hsp90 inhibitors, GA and tanespimycin, has been observed in cultured cancer cells with increased levels of the cystine-glutamate transporter SLC7A11[41] and reduced expression of NAD(P)H/quinone oxidoreductase 1,[42] respectively. Therefore, it has become an urgent matter either to modify known Hsp90 inhibitors or to discover new Hsp90 inhibitors to overcome chemoresistance. Alternatively, targeting the PPI of CCT-β with its substrates (e.g., β-tubulin) may represent a more promising strategy to overcome chemoresistance of Hsp90 inhibitors, as Hsp90 acts as a downstream effector of CCT-β signaling. This concept is supported by microarray analysis displaying that CCT-β mRNA levels in tanespimycin-resistant cancer cell lines are significantly higher than those in tanespimycin-sensitive cells (Supplementary Figure 6).

Recently, the upregulation of VCP expression has been observed in clinical tumors and correlates with both cancer progression and the poor prognosis of cancer patents.[43,44] Moreover, the induction of VCP proteolysis[45] or inhibition of its ATPase activity[13,46] has also been recommended as new chemotherapeutic strategy for cancer therapy. In this study, our data show that the combination of I-Trp and the VCP inhibitor exhibits synergistically cytotoxic effects on the target cells, thereby providing evidence of a PPI inhibitor of the β-tubulin:CCT-β complex in cancer treatment using VCP inhibitor-based chemotherapy. Notably, the understanding of VCP regulation in the targeting of the β-tubulin:CCT-β complex sheds light on the mechanism of overcoming the inefficiency (e.g., chemoresistance) of VCP-targeted chemotherapy.

PTX, an anticancer tubulin-binding agent, targets β-tubulin to impede microtubule dynamics and thereby inhibits tumor growth.[15] However, the alteration of β-tubulin subtype expression,[47,48] especially β-tubulin class III, or the mutation of β-tubulin[49] substantially reduces the anticancer effectiveness of PTX and other taxane derivatives. The Cys^{354}-

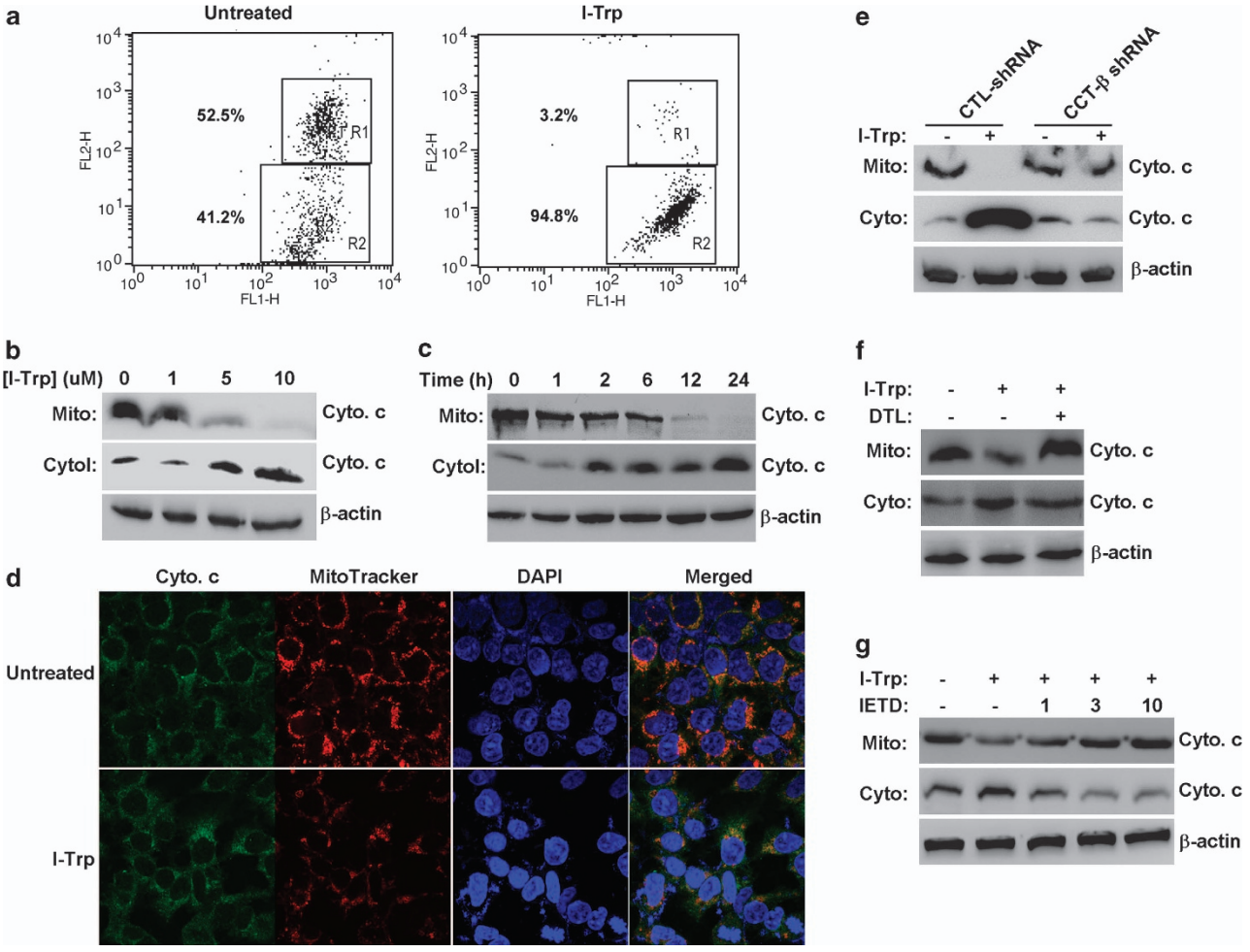

Figure 7 The regulation of I-Trp-induced mitochondrial perturbation. (**a**) I-Trp treatment alters the membrane potential of the mitochondria in HEK-293 cells. Cells either untreated or treated with I-Trp (5 μM) for 2 h were assessed for mitochondrial membrane potential. FL-1 and FL-2 represent the green and red fluorescence channels on the flow cytometer, respectively. The regions R1 and R2 denote the JC-1 aggregates and monomers, respectively. The values indicate the proportion of the cell population in the detected cells. (**b**) I-Trp induces cytochrome *c* (Cyto *c*) release from the mitochondria to the cytoplasm in HEK-293 cells. The Cyto *c* levels were detected in the mitochondrial (Mito.) and cytosol (Cyto.) fractions derived from the cells treated with I-Trp at the indicated concentrations for 24 h by western blot analysis using a specific antibody. (**c**) The Cyto *c* levels were detected by immunoblotting using a specific antibody for the mitochondrial and cytosol fractions derived from the cells treated with 5 μM I-Trp for the designated time periods. (**d**) The cells either untreated or treated with 5 μM I-Trp for 6 h were fixed and stained with Cyto *c* antibody, followed by incubation with FITC (green)-labeled secondary antibody. The cells were further stained with MitoTracker (red) and DAPI (blue) for 15 min before analysis using a confocal microscope. The orange fluorescence denotes the merged fluorescent signals of the FITC-labeled Cyto *c* and the MitoTracker. (**e**) I-Trp-induced Cyto *c* release is affected by CCT-β expression, Ca^{2+} release and caspase-8 activation in HEK-293 cells. The mitochondrial and cytosol fractions derived from the control (CTL) and CCT-β shRNA-expressing HEK-293 cells were treated with 5 μM I-Trp for 24 h. The Cyto *c* levels were assessed by immunoblotting with the corresponding antibody. (**f**) The cells were either untreated or pre-treated with 50 μM DTL for 30 min before the treatment either with or without 5 μM I-Trp. The Cyto *c* levels were measured in the isolated mitochondrial and cytosol fractions 24 h after I-Trp treatment by western blot analysis using the corresponding antibody. (**g**) Cells were pre-incubated either without or with the caspase-8 peptide inhibitor, IETD-CHO, at the indicated doses for 30 min before the treatment either without or with 5 μM I-Trp. The fractionated mitochondrial and cytosol lysates were used to determine the levels of Cyto *c* by immunoblotting. β-Actin expression levels were also assessed by immunoblotting and used as a protein loading CTL for the cytosol fractions

containing sequences VCDIP within the CCT-β-binding interface of β-tubulin are highly conserved among all subtypes[10] and mutant types[49] of β-tubulin, thereby providing the significance of developing PPI inhibitors of the β-tubulin:CCT-β complex to combat taxane-resistant tumors in the clinical setting.

As stated above, the disruption of the β-tubulin:CCT-β complex may represent a promising new strategy to combat MDR cancer cells. In addition to I-Trp and a peptide corresponding to amino acids TAVCDIPPR of β-tubulin that blocks the β-tubulin:CCT-β protein PPI,[10] we have also developed a drug-like small-molecule PPI inhibitor that binds reversibly to β-tubulin in the interface with CCT-β and triggers cell apoptosis via the same mechanism (our unpublished data). Our study therefore unveils signaling pathways useful for developing novel anti-MDR cancer chemotherapy. In summary, targeting the β-tubulin:CCT-β complex elicits ER stress-associated apoptosis via Ca^{2+}-dependent mitochondrial perturbation and caspase overactivation. These findings also represent an advance in the understanding of the PPI of CCT-β with Hsp90-dependent and VCP-centered protein trafficking/degradation systems and the

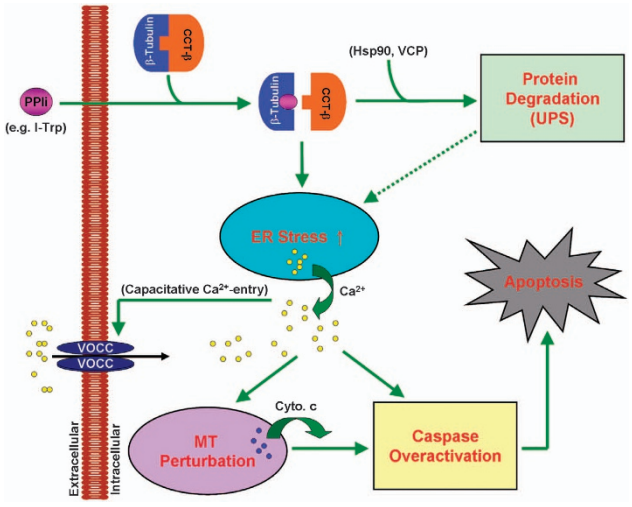

Figure 8 The illustration of the molecular signaling pathway of ER stress-induced cell apoptosis provoked by β-tubulin:CCT-β complex destruction. PPIi and voltage-operated Ca^{2+} channel (VOCC) are the abbreviations for protein–protein interaction inhibitor and voltage-operated Ca^{2+} channels, respectively

XIAP/caspase-7-associated apoptosome, which may provide an alternative option to overcome chemoresistance to Hsp90- and VCP-targeting anticancer agents.

Materials and Methods

Materials. All chemicals used for organic synthesis were purchased from Aldrich-Sigma (St. Louis, MO, USA). MitoTracker and Fura-2-AM were purchased from Invitrogen (Carlsbad, CA, USA). Protein A-agarose; antibodies against β-tubulin, β-actin, CCT-β, cytochrome *c* and Hsp90; siRNA for VCP; and shRNA for CCT-β and Hsp90 were purchased from Santa Cruz Biotechnology (Santa Cruz, CA, USA). Antibodies against VCP, ubiquitin and GAPDH were purchased from Cell Signaling (Danvers, MA, USA). TG, DTL and BAPTA were purchased from Calbiochem (San Diego, CA, USA). Mitochondrial membrane potential detection kits were obtained from BD Biosciences (San Jose, CA, USA). Caspase and proteasome activity assay kits, GA and the caspase-8 inhibitor were purchased from BioVision (Mountain View, CA, USA). The VCP inhibitor (patent no: CIT-5066) was generously provided by Dr. Chou TF at the California Institute of Technology (Pasadena, CA, USA).

Cell culture. All cell lines used in this study were obtained from the Bioresource Collection and Research Center in Taiwan. HEK-293 cells were cultivated in MEM supplemented with 10% fetal bovine serum (FBS) and 250 U/ml of penicillin/streptomycin solution. MES-SA and MES-SA/Dx-5 uterine cancer cells were cultivated in McCoy's 5A medium supplemented with 10% FBS and 250 U/ml of penicillin/streptomycin solution. All cell culture media and supplements were purchased from Gibco (Invitrogen). The cells were maintained in the presence of 5% CO_2 at 37 °C.

Plasmid construction and protein expression. The genes encoding CCT-β (NM_006431.2), β-tubulin (NM_006087.2) and VCP (NM_007126.2) were amplified from human cDNA (Invitrogen) using the standard or sticky-end polymerase chain reaction (PCR) procedure with paired primers (See Supplementary Table 1) and subcloned into either the pET32-Xa/LIC (for CCT-β) or pIRES2-EGFP (for β-tubulin and VCP) vectors, respectively. The pIRES2-EGFP/β-tubulin plasmid was used as a DNA template for site-directed mutagenesis of the Cys^{354} residue to Ser. The PCR reaction was performed using paired primers (see Supplementary Table 1) and a Pfu polymerase kit (Stratagene, Cedar Creek, TX, USA). The PCR products were treated with *Dpn*1 endonuclease (New England BioLabs, Ipswich, MA, USA) to digest the methylated parental DNA template. The identities of individual clones were verified via double-strand plasmid sequencing.

Recombinant CCT-β was overexpressed in the *Escherichia coli* strain BL-21(DE3) as a C-terminal hexa-His-tagged protein. To generate stable cell lines, HEK-293 cells were transfected for 24 h with pIRES2-EGFP plasmid DNA with or without either β-tubulin or the *VCP* gene at 1 μg using the Lipofetamine delivery system (Invitrogen). After selection with G418 antibiotic, cells were seeded in 96-well plates at a density of 5 cells per ml to yield a single colony per well. Cells stably expressing either the β-tubulin or VCP constructs were monitored by EGFP expression.

Protein purification. Protein purification was performed at 4 °C. Cell pellets obtained from a 2-l culture of the *E. coli* strain BL-21(DE3) were resuspended in 80 ml buffer A (12 mM Tris-HCl (pH 7.5) and 120 mM NaCl). A French pressure cell (AIM-AMINCO Spectronic Instruments, Lake Forest, NY, USA) was used to disrupt the cells at 12 000 psi. Cell lysates were centrifuged at 25 000 $\times$ *g* at 4 °C. Supernatants were loaded onto a 20 ml Ni-NTA resin that was equilibrated with buffer A. The column was washed with excess buffer A containing 10 mM imidazole. His-tagged CCT-β was eluted with buffer B (12 mM Tris-HCl (pH 7.5), 120 mM NaCl and 300 mM imidazole). The eluted protein solution was dialyzed with 2 $\times$ concentrated buffer A at 4 °C overnight.

siRNA transfection and lentivirus-driven shRNA infection. Cells (50% confluence) grown in 6-well plates were transfected with either control or VCP siRNA at 100 nM for 24 h before observing cellular vacuolization or bathed in fresh media containing 5 μg/ml of polybrene (Santa Cruz Biotechnology) before infection with a lentiviral viral particle-driven control, CCT-β or Hsp90 shRNA overnight. To select cells stably expressing the control, CCT-β or Hsp90 shRNA, cells were cultivated in the presence of puromycin (10 μg/ml) for 24 h. The puromycin-resistant cells were subsequently split into 96-well plates at a density of 1 cell per well to generate a cell line stably expressing the control, CCT-β or Hsp90 shRNA.

Preparation of cytosolic and mitochondrial fractions. Cells were collected in 1 ml hypotonic HEPES buffer (10 mM HEPES (pH 7.4), 5 mM $MgCl_2$, 40 mM KCl and 4% protease inhibitor cocktail (Merck Biosciences, San Diego, CA, USA)) and placed on ice for 30 min. Cell suspensions were passed through a 27-G needle-containing syringe 25 times before the centrifugation at 1000 $\times$ *g* for 20 min. The supernatants were further centrifuged at 10 000 $\times$ *g* for 30 min to separate the cytosolic fractions (supernatants) from the mitochondrial fractions (pellets).

Western blotting. The cell lysates (100 μg) were boiled for 5 min in SDS sample buffer (62.5 mM Tris-HCl (pH 6.7), 1.25% SDS, 12.5% glycerol and 2.5% β-mercaptoethanol) and the proteins were separated via SDS-PAGE. For western blotting, proteins were transferred onto a PVDF membrane (Millipore, Billerica, MA, USA) and incubated with an antibody against ubiquitin, β-tubulin, CCT-β, Hsp90, VCP, cytochrome *c*, GAPDH or β-actin. After incubation with horseradish peroxidase-conjugated secondary antibody, immunoreactive protein bands were visualized using the enhanced chemiluminescence system (Amersham Bioscience, Tokyo, Japan).

RT-PCR. Total RNA was extracted from cells using a RNA extraction kit (Genomics, Taipei, Taiwan). Aliquots (5 μg) of total RNA were treated with M-MLV reverse transcriptase (Invitrogen) and then amplified with *Taq* polymerase (MDBIO, Beijing, China) using paired primers as shown in Supplementary Table 1.

Apoptosis assessment. Cells (6×10^5) were fixed in 70% ice-cold EtOH for 30 min at RT. Cells were washed with PBS once and were incubated with propidium iodide (PI) staining solution (PBS containing 0.1% BSA, 0.1% RNase A and 20 ng/ml PI) for 30 min at RT in the dark. After the incubation, the cells were analyzed by flow cytometry to assess their DNA content. Cells accumulated in the sub-G0 region were defined as apoptotic cells because we have verified that the cytotoxic effects of I-Trp on HEK-293 cells is via apoptotic cell death, as determined by DNA fragmentation.[10]

Determination of proteasome activity. After being treated with I-Trp (5 μM) for designated time periods, cells were collected and resuspended in cell lysis buffer (BioVision). Aliquots of cell lysates (50 μg) were incubated with 1 μM of fluorescent proteasome substrate (BioVision) for 30 min at 37 °C. The fluorescent intensity was read using a fluorimeter with an exciting wavelength at 355 nm and emission wavelength at 405 mm and presented as relative proteasomal activity.

Mass spectrometric analysis. Protein bands A, B and C (Supplementary Figure 2c) were excised from the gel and subject to in-gel tryptic digestion and liquid chromatography-electrospray ionization-tandem mass spectrometric analysis. The raw data were converted to the Mascot (Matrix Science) generic format and analyzed using the NCBInr human protein database.

Calcium image. Cells were seeded on poly-L-lysine-coated round cover slides (22 mm in diameter and 0.17 mm in thickness). After a 2-day culture, cells were pre-incubated with 4 μM Fluoro-3 dye at 37 °C for 30 min. After incubation, cells were transferred to a slide chamber containing 0.4 ml Hank's balanced saline solution and examined using a confocal microscope (Olympus, Tokyo, Japan) with an argon laser (488 nm). After adjusting the proper field, I-Trp (5 μM) was carefully added into the slide chamber, and the changes in intracellular Ca^{2+} levels were observed.

Measurement of intracellular calcium. Cells were cultured in 6-well culture plates containing poly-L-lysine-coated $9 \times 220\ mm^2$ cover slides. After a 2-day culture, cells were pre-treated with 5 μM Fura-2-AM for 30 min at 37 °C. Subsequently, each cell-grown cover slide was transferred into a 4-ml quartz cuvette containing 2 ml focal buffer (10 mM HEPES, 140 mM NaCl, 5 mM KCl and 2.6 mM D-glucose). The analysis of the intracellular calcium oscillation was performed using a Hitachi F-4500 Fluorescence Spectrophotometer with the Intracellular Cation Measurement System (Hitachi, Tokyo, Japan). A designated amount of I-Trp (5 μM), IDAM (5 μM) or TG (1 μM) was added using a microinjection syringe when the baseline (380 nm) was stable. The levels of intracellular calcium are presented by the ratio of 340- to 380-nm excitation wavelength-induced fluorescent intensities emitted at 510 nm.

Determination of the mitochondrial membrane potential. HEK-293 cells (5×10^6) were collected post-treatment with or without I-Trp (5 μM) for 2 h at 37 °C and stained with JC-1 working solution (BD Biosciences) for 15 min at RT. After washing the cells with assay buffer (BD Biosciences) two times, the cells were resuspended in 0.5-ml assay buffer and analyzed via flow cytometry. JC-1 is a lipophilic fluorochrome that is used to evaluate the status of the membrane potential ($\Delta\psi$) and driven into the mitochondria by $\Delta\psi$. JC-1 is rapidly taken up by the cell and forms aggregates within the healthy mitochondria. The aggregates can be detected in the red (FL-2) channel on the flow cytometer. In contrast, JC-1 does not accumulate within the mitochondria with depolarized $\Delta\psi$ and remains in the cytoplasm as monomers and therefore displays a reduced fluorescence in the FL-2 channel.

Confocal microscope observation. Cells (1×10^5/ml) cultivated on cover slides (22 mm in diameter and 0.17 mm in thickness) were fixed in 4% formaldehyde for 15 min at RT. After washing cells two times with PBS, the cells were treated with 95% EtOH/5% CH_3COOH at -20 °C for 15 min. Before blocking with 2% BSA/0.1% Triton X-100 for 2 h at RT, the cells were washed two times with PBS. Subsequently, the cells were incubated with cytochrome *c* antibody overnight at 4 °C. After washing the cells three times with PBS, the cells were incubated with biotin-conjugated secondary antibody (DAKO, Glostrup, Denmark) for 1 h at RT. The cells were washed three times with PBS and incubated with fluorescein-conjugated avidin complex (Vector Laboratories, Peterborough, UK) for 30 min at RT. For mitochondrial staining, cells were incubated with MitoTracker (Invitrogen) for another 15 min at RT. After mounting the cells with a commercial kit containing DAPI reagent (Vector Laboratories), the cells were analyzed using a FluoView confocal microscope system (Olympus).

Determination of caspase activity. The caspase activity assay was performed according to the manufacturer's guidelines (BioVision). Briefly, cell lysates (200 μg) were diluted in 50 μl of cell lysis buffer (supplied by the kit). Equal volumes of the 2 $\times$ reaction buffer (supplied by the kit) containing 10 mM DTT were added to the cell lysates. Subsequently, 50 μM of fluorescent dye-conjugated caspase substrate was individually added to the designated caspase activity assay. After a 2-h incubation, free fluorescent dyes in the solution were read in a fluorimeter equipped with a 385- and 510-nm emission filter. Fold increases in caspase activity were determined by comparing these results with the level of the untreated control.

Statistical analysis. In this study, statistical analysis of three independent experiments was performed using the non-parametric Mann–Whitney test. All statistical tests were two-sided, and $P < 0.05$ was considered to be significant ($^*P < 0.05$, $^{**}P < 0.01$ and $^{***}P < 0.001$).

Conflict of Interest

The authors declare no conflict of interest.

Acknowledgements. We thank Dr. Raymond J Deshaies and Dr. Tsui-Fen Chou for generously providing the VCP inhibitors, Miss Yi-An Chou for her assistance in generating stable cell lines, and Mr. Vathan Kumar for synthesizing the I-Trp compound.

Author contributions

Lin Y-F performed most of the experiments and wrote the manuscript. Lee Y-F performed the CCT-β pull-down assay, the caspase activity analysis, and the determination of cytochrome *c* release. Liang P-H designed and supervised all aspects of the research and finalized the article.

1. Llorca O, Martín-Benito J, Gómez-Puertas P, Ritco-Vonsovici M, Willison KR, Carrascosa JL *et al.* Analysis of the interaction between the eukaryotic chaperonin CCT and its substrates actin and tubulin. *J Struct Biol* 2001; **135**: 205–218.
2. Dekker C, Stirling PC, McCormack EA, Filmore H, Paul A, Brost RL *et al.* The interaction network of the chaperonin CCT. *EMBO J* 2008; **27**: 1827–1839.
3. Rivenzon-Segal D, Wolf SG, Shimon L, Willison KR, Horovitz A. Sequential ATP-induced allosteric transitions of the cytoplasmic chaperonin containing TCP-1 revealed by EM analysis. *Nat Struct Mol Biol* 2005; **12**: 233–237.
4. Grantham J, Brackley KI, Willison KR. Substantial CCT activity is required for cell cycle progression and cytoskeletal organization in mammalian cells. *Exp Cell Res* 2006; **312**: 2309–2324.
5. Brackley KI, Grantham J. Activities of the chaperonin containing TCP-1 (CCT): implications for cell cycle progression and cytoskeletal organisation. *Cell Stress Chaperones* 2009; **14**: 23–31.
6. Posokhova E, Song H, Belcastro M, Higgins L, Bigley LR, Michaud NA *et al.* Disruption of the chaperonin containing TCP-1 function affects protein networks essential for rod outer segment morphogenesis and survival. *Mol Cell Proteomics* 2011; **10**: M110.
7. Qian-Lin Z, Ting-Feng W, Qi-Feng C, Min-Hua Z, Ai-Guo L. Inhibition of cytosolic chaperonin CCTzeta-1 expression depletes proliferation of colorectal carcinoma *in vitro*. *J Surg Oncol* 2010; **102**: 419–423.
8. Yokota S, Yamamoto Y, Shimizu K, Momoi H, Kamikawa T, Yamaoka Y *et al.* Increased expression of cytosolic chaperonin CCT in human hepatocellular and colonic carcinoma. *Cell Stress Chaperones* 2001; **6**: 345–350.
9. Coghlin C, Carpenter B, Dundas SR, Lawrie LC, Telfer C, Murray GI. Characterization and over-expression of chaperonin t-complex proteins in colorectal cancer. *J Pathol* 2006; **210**: 351–357.
10. Lin YF, Tsai WP, Liu HG, Liang PH. Intracellular beta-tubulin/chaperonin containing TCP1-beta complex serves as a novel chemotherapeutic target against drug-resistant tumors. *Cancer Res* 2009; **69**: 6879–6888.
11. Mimnaugh EG, Xu W, Vos M, Yuan X, Neckers L. Endoplasmic reticulum vacuolization and valosin-containing protein relocalization result from simultaneous hsp90 inhibition by geldanamycin and proteasome inhibition by velcade. *Mol Cancer Res* 2006; **4**: 667–681.
12. Wojcik C, Rowicka M, Kudlicki A, Nowis D, McConnell E, Kujawa M *et al.* Valosin-containing protein (p97) is a regulator of endoplasmic reticulum stress and of the degradation of N-end rule and ubiquitin-fusion degradation pathway substrates in mammalian cells. *Mol Biol Cell* 2006; **17**: 4606–4618.
13. Chou TF, Brown SJ, Minond D, Nordin BE, Li K, Jones AC *et al.* Reversible inhibitor of p97, DBeQ, impairs both ubiquitin-dependent and autophagic protein clearance pathways. *Proc Natl Acad Sci USA* 2011; **108**: 4834–4839.
14. Whitesell L, Lin NU. HSP90 as a platform for the assembly of more effective cancer chemotherapy. *Biochim Biophys Acta* 2012; **1823**: 756–766.
15. Vyas DM, Kadow JF. Paclitaxel: a unique tubulin interacting anticancer agent. *Prog Med Chem* 1995; **32**: 289–337.
16. Shin JH, Kim HW, Rhyu IJ, Song KJ, Kee SH. Axin expression reduces staurosporine-induced mitochondria-mediated cell death in HeLa cells. *Exp Cell Res* 2012; **318**: 2022–2033.
17. Taipale M, Jarosz DF, Lindquist S. HSP90 at the hub of protein homeostasis: emerging mechanistic insights. *Nat Rev Mol Cell Biol* 2010; **11**: 515–528.
18. Dahlmann B, Kuehn L. The 20S/26S proteasomal pathway of protein degradation in muscle tissue. *Mol Biol Rep* 1995; **21**: 57–62.
19. Ye Y, Meyer HH, Rapoport TA. Function of the p97–Ufd1–Npl4 complex in retrotranslocation from the ER to the cytosol: dual recognition of nonubiquitinated polypeptide segments and polyubiquitin chains. *J Cell Biol* 2003; **162**: 71–84.
20. Pearce MM, Wormer DB, Wilkens S, Wojcikiewicz RJ. An endoplasmic reticulum (ER) membrane complex composed of SPFH1 and SPFH2 mediates the

ER-associated degradation of inositol 1,4,5-trisphosphate receptors. *J Biol Chem* 2009; **284**: 10433–10445.
21. Deveraux QL, Takahashi R, Salvesen GS, Reed JC. X-linked IAP is a direct inhibitor of cell-death proteases. *Nature* 1997; **388**: 300–304.
22. Hiscutt EL, Hill DS, Martin S, Kerr R, Harbottle A, Birch-Machin M *et al.* Targeting X-linked inhibitor of apoptosis protein to increase the efficacy of endoplasmic reticulum stress-induced apoptosis for melanoma therapy. *J Invest Dermatol* 2010; **130**: 2250–2258.
23. Jang M, Park BC, Lee AY, Na KS, Kang S, Bae KH *et al.* Caspase-7 mediated cleavage of proteasome subunits during apoptosis. *Biochem Biophys Res Commun* 2007; **363**: 388–394.
24. Saini RV, Wilson C, Finn MW, Wang T, Krensky AM, Clayberger C. Granulysin delivered by cytotoxic cells damages endoplasmic reticulum and activates caspase-7 in target cells. *J Immunol* 2011; **186**: 3497–3504.
25. Cuellar J, Martín-Benito J, Scheres SH, Sousa R, Moro F, López-Viñas E *et al.* The structure of CCT-Hsc70 NBD suggests a mechanism for Hsp70 delivery of substrates to the chaperonin. *Nat Struct Mol Biol* 2008; **15**: 858–864.
26. Weis F, Moullintraffort L, Heichette C, Chretien D, Garnier C. The 90-kDa heat shock protein Hsp90 protects tubulin against thermal denaturation. *J Biol Chem* 2010; **285**: 9525–9534.
27. Zhong X, Shen Y, Ballar P, Apostolou A, Agami R, Fang S *et al.* AAA ATPase p97/valosin-containing protein interacts with gp78, a ubiquitin ligase for endoplasmic reticulum-associated degradation. *J Biol Chem* 2004; **279**: 45676–45684.
28. Wojcik C, Yano M, DeMartino GN. RNA interference of valosin-containing protein (VCP/p97) reveals multiple cellular roles linked to ubiquitin/proteasome-dependent proteolysis. *J Cell Sci* 2004; **117**: 281–292.
29. Yoshida H, Matsui T, Yamamoto A, Okada T, Mori K. XBP1 mRNA is induced by ATF6 and spliced by IRE1 in response to ER stress to produce a highly active transcription factor. *Cell* 2001; **107**: 881–891.
30. Kim HR, Kim MS, Kwon DY, Chae SW, Chae HJ. Bosellia serrata-induced apoptosis is related with ER stress and calcium release. *Genes Nutr* 2008; **2**: 371–374.
31. Thastrup O, Dawson AP, Scharff O, Foder B, Cullen PJ, Drøbak BK *et al.* Thapsigargin, a novel molecular probe for studying intracellular calcium release and storage. 1989. *Agents Actions* 1994; **43**: 187–193.
32. Cameron EM, Zhuang J, Menconi MJ, Phipps R, Fink MP. Dantrolene, an inhibitor of intracellular calcium release, fails to increase survival in a rat model of intra-abdominal sepsis. *Crit Care Med* 1996; **24**: 1537–1542.
33. Zhou S, Yuan X, Liu Q, Zhang X, Pan X, Zang L *et al.* BAPTA-AM, an intracellular calcium chelator, inhibits RANKL-induced bone marrow macrophages differentiation through MEK/ERK, p38 MAPK and Akt, but not JNK pathways. *Cytokine* 2010; **52**: 210–214.
34. Gonzalez D, Espino J, Bejarano I, López JJ, Rodríguez AB, Pariente JA. Caspase-3 and -9 are activated in human myeloid HL-60 cells by calcium signal. *Mol Cell Biochem* 2010; **333**: 151–157.
35. Hom JR, Gewandter JS, Michael L, Sheu SS, Yoon Y. Thapsigargin induces biphasic fragmentation of mitochondria through calcium-mediated mitochondrial fission and apoptosis. *J Cell Physiol* 2007; **212**: 498–508.
36. Kantari C, Walczak H. Caspase-8 and bid: caught in the act between death receptors and mitochondria. *Biochim Biophys Acta* 2011; **1813**: 558–563.
37. Pascale RM, Simile MM, Calvisi DF, Frau M, Muroni MR, Seddaiu MA *et al.* Role of HSP90, CDC37, and CRM1 as modulators of P16(INK4A) activity in rat liver carcinogenesis and human liver cancer. *Hepatology* 2005; **42**: 1310–1319.
38. Milicevic Z, Bogojevic D, Mihailovic M, Petrovic M, Krivokapic Z. Molecular characterization of hsp90 isoforms in colorectal cancer cells and its association with tumour progression. *Int J Oncol* 2008; **32**: 1169–1178.
39. Sydor JR, Normant E, Pien CS, Porter JR, Ge J, Grenier L *et al.* Development of 17-allylamino-17-demethoxygeldanamycin hydroquinone hydrochloride (IPI-504), an anti-cancer agent directed against Hsp90. *Proc Natl Acad Sci USA* 2006; **103**: 17408–17413.
40. Fukuyo Y, Hunt CR, Horikoshi N. Geldanamycin and its anti-cancer activities. *Cancer Lett* 2010; **290**: 24–35.
41. Liu R, Blower PE, Pham AN, Fang J, Dai Z, Wise C *et al.* Cystine-glutamate transporter SLC7A11 mediates resistance to geldanamycin but not to 17-(allylamino)-17-demethoxygeldanamycin. *Mol Pharmacol* 2007; **72**: 1637–1646.
42. Gaspar N, Sharp SY, Pacey S, Jones C, Walton M, Vassal G *et al.* Acquired resistance to 17-allylamino-17-demethoxygeldanamycin (17-AAG, tanespimycin) in glioblastoma cells. *Cancer Res* 2009; **69**: 1966–1975.
43. Yamamoto S, Tomita Y, Nakamori S, Hoshida Y, Iizuka N, Okami J *et al.* Valosin-containing protein (p97) and Ki-67 expression is a useful marker in detecting malignant behavior of pancreatic endocrine neoplasms. *Oncology* 2004; **66**: 468–475.
44. Yamamoto S, Tomita Y, Hoshida Y, Takiguchi S, Fujiwara Y, Yasuda T *et al.* Expression level of valosin-containing protein is strongly associated with progression and prognosis of gastric carcinoma. *J Clin Oncol* 2003; **21**: 2537–2544.
45. Guo Y, Chen J, Shi L, Fan Z. Valosin-containing protein cleavage by granzyme K accelerates an endoplasmic reticulum stress leading to caspase-independent cytotoxicity of target tumor cells. *J Immunol* 2010; **185**: 5348–5359.
46. Bursavich MG, Parker DP, Willardsen JA, Gao ZH, Davis T, Ostanin K *et al.* 2-Anilino-4-aryl-1,3-thiazole inhibitors of valosin-containing protein (VCP or p97). *Bioorg Med Chem Lett* 2010; **20**: 1677–1679.
47. Burkhart CA, Kavallaris M, Band HS. The role of beta-tubulin isotypes in resistance to antimitotic drugs. *Biochim Biophys Acta* 2001; **1471**: O1–O9.
48. Umezu T, Shibata K, Kajiyama H, Terauchi M, Ino K, Nawa A *et al.* Taxol resistance among the different histological subtypes of ovarian cancer may be associated with the expression of class III beta-tubulin. *Int J Gynecol Pathol* 2008; **27**: 207–212.
49. Yin S, Cabral F, Veeraraghavan S. Amino acid substitutions at proline 220 of beta-tubulin confer resistance to paclitaxel and colcemid. *Mol Cancer Ther* 2007; **6**: 2798–2806.

Supplementary Information accompanies the paper on Cell Death and Disease website (http://www.nature.com/cddis)